Lakhe et al., J Material Sci Eng 2016, 5:4
DOI: 10.4172/2169-0022.1000261

Journal of Material Science & Engineering

Research Article Open Access

Electrochemical Synthesis and Characterization of Cu_2ZnSnS_4 Thin Films

Lakhe MG, Bhand GR, Londhe PU, Rohom AB and Chaure NB*

Electrochemical Laboratory, Department of Physics, Savitribai Phule Pune University, India

Abstract

Cu_2ZnSnS_4 (CZTS) thin films have been electrochemically deposited from aqueous electrolyte containing $CuCl_2$, $ZnCl_2$, $SnCl_4$ and $Na_2S_2O_3$ onto fluorine doped tin oxide (FTO) coated glass substrates. A conventional three-electrode geometry consisting working, counter and reference electrodes was used to perform the electrochemical experiments. The films were deposited at - 1.1 V with respect to Ag/AgCl reference, which was optimized by cyclic voltammetry. CZTS layers were annealed in tubular furnace at 400°C for 15 minutes in vacuum. As-deposited and annealed CZTS films were characterized using range of characterization techniques to study the structural, optical, morphological, and compositional and optoelectronic properties. Annealed sample revealed (112), (220) and (312) planes corresponds to tetragonal kesterite CZTS structure and secondary peaks of CuZn alloy. The optical study shows that the band gap of the as-deposited CZTS film was found to be 1.68 eV. Upon annealing the optical band gap ~ 1.49 eV corresponds to CZTS were estimated from UV-Visible Spectroscopy and photoluminescence. Densely packed, void free and relatively uniform thin films were deposited by electrodeposition technique. The grain size has been increased upon the heat treatment. Copper and zinc rich off-stoichiometric films were deposited at -1.1 V. Current density-Voltage (J-V) measurements showed Schottkey behavior. The flat band potential and carrier concentration estimated by C-V measurement for annealed CZTS sample was 0.30 V and ~ 2.4 x 10^{16} cm^{-3} respectively.

Keywords: CZTS thin films; Kesterite structure; Cyclic voltammetry; Characterization

Introduction

It is important to fabricate thin film solar cells with high efficiency from earth abundant, non-toxic and environmentally friendly elements/materials. In this scenario $Cu_2ZnSnSe/S_4$ (CZTSe/S) brings new hopes. It is I_2–II–IV–VI_4 promising quaternary kesterite non-toxic semiconducting compound with p-type conductivity [1-5] and large absorption coefficient, 10^4 cm^{-1} [2]. Its optical band gap varies from 1.0 eV to 1.5 eV [1-5] by replacing selenium with sulphur. The highest reported efficiency is 12.6% [6]. It can be synthesized by number of techniques such as hydrazine based solution process [7-9], nanoparticles from nontoxic solutions [10], thermal evaporation [11-13], chemical vapor deposition [14], sputtering [15-18], e-beam evaporation [19], electrodeposition using ionic liquids [20-25], spray pyrolysis [26,27] etc. Electrodeposition is one of the easy, scalable, cost-effective and found to be very successful technique. Either single-step or multistep approach has been accepted for the electrodeposition of CZTS absorber layer. Slupska et al. [28] has grown Sn-Zn-Cu alloy from aqueous bath containing $CuSO_4$, $SnSO_4$ and $ZnSO_4$ precursors by electrodeposition technique. Tri-sodium citrate was used as complexing agent/supportive electrolyte. Khalil et al. [29] has deposited Cu-Zn-Sn metal alloys on molybdenum substrate from electrolyte containing $CuSO_4$, $ZnSO_4$, Na_2SnO_3 and $K_4P_2O_7$. CZT alloy thin films were subsequently annealed in elemental sulphur ambient for the formation of CZTS. Valdes et al. [30] has electrodeposited CZTS thin films by electrochemical atomic layer deposition and conventional one-step electrodeposition. The deposition of non-stoichiometric CZTS films is reported by one-step electrodeposition. Here we report the synthesis of Cu_2ZnSnS_4 (CZTS) onto FTO substrate by single-step electrodeposition from aqueous bath. The preliminary results obtained from the pristine and annealed thin films are discussed.

Experimental Details

The CZTS films have been synthesized on FTO substrate by cathodic potentiostatic electrodeposition technique at pH 4.5 and bath temperature 50°C with moderate stirring. $CuCl_2$, $ZnCl_2$, $SnCl_2$ and $Na_2S_2O_3$ were used as precursors for the co-deposition of Cu, Zn, Sn and S, respectively. Tri-sodium citrate is used as complexing agent for the stoichiometric co-deposition of precursors [23,28,30-32]. A standard three-electrode system consisting working, counter and reference electrodes was employed for the electrodeposition of CZTS films. Commercially available fluorine doped tin oxide (FTO) coated soda lime glass substrates of resistivity 10-15 Ω/sq, platinum sheet and Ag/AgCl were used as working, counter and reference electrode, respectively. Potentiostat/galvanostat Model, Biologic SP 300 was used to perform the cyclic voltammetry (CV) and electrodeposition of CZTS thin films. Prior to the experimentation, all substrates were thoroughly cleaned using double distilled boiled water, acetone and iso-propanol followed by few minutes ultra-sonication with iso-propanol. The CV experiments were performed for various bath temperatures and stirring rate to optimize the suitable deposition potential for co-deposition of Cu, Zn, Sn and S. Deposition potential -1.1 V was optimized by using cyclic voltammetry experiments. The samples were annealed in vacuum at 400°C for 15 minutes. The pristine and annealed samples were studied by range of characterization techniques to study structural, optical, morphological, compositional and electrical properties. X-ray diffractometer (Model Bruker D8 Advance, Germany) of Cu Kα radiation, with λ=0.154 nm was used to study the structural properties. Optical measurements were performed using JASCO, UV-VIS-NIR Spectrophotometer model V-670. Photoluminescence was studied by

***Corresponding author:** Chaure NB, Electrochemical Laboratory, Department of Physics, Savitribai Phule Pune University, India, Tel: 912025699072; Fax: 912025691684; E-mail: n.chaure@physics.unipune.ac.in

Received May 13, 2016; **Accepted** June 01, 2016; **Published** June 11, 2016

Citation: Lakhe MG, Bhand GR, Londhe PU, Rohom AB, Chaure NB (2016) Electrochemical Synthesis and Characterization of Cu_2ZnSnS_4 Thin Films. J Material Sci Eng 5: 261. doi:10.4172/2169-0022.1000261

Perkin Elmer LS-55 Spectrophotometer. JEOL JSM-6360 A SEM/EDAX at accelerating voltage 20 kV and probe current 1 nA was used to study the surface morphology and elemental composition. Current density-Voltage (J-V) measurements were performed using the Potentiostat/galvanostat Model, Biologic SP 300. Frequency response analyzer (FRA) facility available in above mentioned potentiostat was used to study the C-V measurements at frequency 100 KHz.

Results and Discussion

Cyclic voltammetry

The cyclic voltammogram recorded with respect to Ag/AgCl reference electrode in the bath consisting precursors of Cu, Zn, Sn and S is shown in Figure 1. The temperature of the bath was maintained at 50°C with continuous stirring with 180 rpm throughout the experimentation. The redox potentials of Cu, Zn, Sn and S are different; therefore the co-deposition of these elements is difficult. However with the help of complexing agent the stoichiometric deposition can be obtained. The complexing agent can slow down the rate of reaction by forming complex or ligands with the nobel ionic species. The cathodic and anodic curves are marked by forward (black) and reverse (red) arrows. During the cathodic scan, upto ~ - 0.6 V, current was nearly steady indicates the applied growth potential was not sufficienct to deposite the precursors. The current found to be increased beyond -0.6 V to -0.9 V could be due to the metallic deposition of copper and zinc. The small plateau region revealed around – 1.0 V to -1.1 V ('A') could be suitable for the co-deposition of CZTS. The sharp linear rise in current beyond -1.1 V is proposed due to the rapid growth of metallic Cu_xZn_y alloy along with hydrogen evolution. The peak attributed during the anodic scan about -0.30 V, -0.15 V and + 0.30 V are associated to the stripping of Zn, Sn and Cu respectively. Indeed, we observed that the layer was completely stripped out after complition of CV measurement.

The flow of the complexed ionic species towards the electrode was maintained with continuous stirring. The number of samples

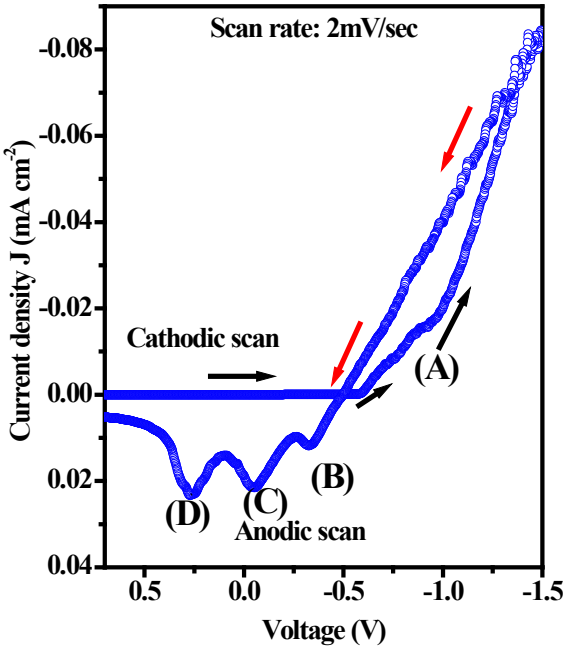

Figure 1: Cyclic voltammogram recorded at 50°C on FTO substrate in electrolyte containing Cu, Zn, Sn and S ionic species at pH 4.5.

were scanned during cyclic voltammetry experiment to optimize the deposition potential and it was found to be ~ - 1.1 V with respect to Ag/AgCl reference electrode. The reduction of copper, zinc, tin and sulphur occurs by the following reaction mechanism [33];

$$Cu^{2+} + 2e^- \rightarrow Cu_{(S)} \quad (1)$$

$$Zn^{2+} + 2e^- \rightarrow Zn_{(S)} \quad (2)$$

$$Sn^{2+} + 2e^- \rightarrow Sn_{(S)} \quad (3)$$

The deposition of sulphur is not straight forward. In the present bath $SnCl_2$ and $Na_2S_2O_3$ are used as sources of Sn and S respectively. Both the sources are strong reducing agents which can reduce the copper and zinc; therefore copper and zinc rich layers can be deposited. Upon the application of deposition potential $Na_2S_2O_3$ may decomposes by the following reaction mechanism,

$$Na_2S_2O_3 \rightarrow Na^{2+} + S_2O_3^{2-} \quad (4)$$

The $S_2O_3^{2-}$ reacts with the ligands of the Cu and Zn and directly get deposited on the substrate in the form of CuS or ZnS. Another possible mechanism is, $S_2O_3^{2-}$ reacts with the CuZn metallic species which was already deposited on substrate and sulfurization occurs on the upper surface only which leads to the metal rich graded deposition of CZTS on the CuZn surface. The reported reduction potential for Cu, Zn and Sn [33] with respect to normal hydrogen are + 0.34 V, -0.763V and -0.136 respectively.

X- ray diffraction

The XRD pattern of (a) as-deposited and (b) annealed CZTS sample is shown in Figure 2. FTO peaks are marked by dark solid circles (•). In as-deposited sample, the two peaks present at 43.26° and 50.15° corresponds to (210) and (020) planes of Cu_5Zn_8, respectively [JCPDF file No. 14-1435]. The broad hump ranging from 20-28° corresponds the mixed amorphous and crystalline nature having short range periodicity of mixed ternary and quaternary phases of CuZnS or CZTS materials.

Upon heat treatment the broad hump is disappeared and the peaks exhibited at 28.58°, 47.61° and 56.71° corresponds to (112), (220) and (312) planes of CZTS of tetragonal kesterite structure [JCPDF file 26-0575]. The transfer of one phase to another phase depends on the formation of enthalpy of the particular phase. An important issue regarding the phase formation with quaternary semiconductors is whether homogeneous samples can be synthesized experimentally, or some secondary phases are also unintentionally formed. People have grown CZTS samples successfully using a variety of techniques (vacuum and non-vacuum; solution and solid-state) reported above, and significant variation has been achieved in the Cu: Zn: Sn atomic ratio, depending on the growth environment. If secondary phases are formed during the synthesis, these phases can be removed upon annealing in inert atmosphere. To describe the phase stability of CZTS as compared to the secondary phases Walsh et al. [34] has calculated the chemical stability region in the atomic chemical potential. To maintain a stable Cu_2ZnSnS_4 crystal, the chemical potentials of Cu, Zn, Sn, and S must satisfy the following equation:

$$2\mu_{Cu} + \mu_{Zn} + \mu_{Sn} + 4\mu_S = \Delta H_f\left(Cu_2ZnSnS_4\right) = -4.21\ eV \quad (5)$$

where ΔH_f represents the formation of enthalpy for CZTS from their respective elements. Both factors i.e., variation of Cu:Zn:Sn:S ratios and annealing treatment controls the chemical potential which shows the stable phase of CZTS within a narrow thermodynamic window.

Secondary phases observed at 42.75° and 49.83° corresponds to CuZn metallic alloy. It is also noticed that depending upon the enthalpy

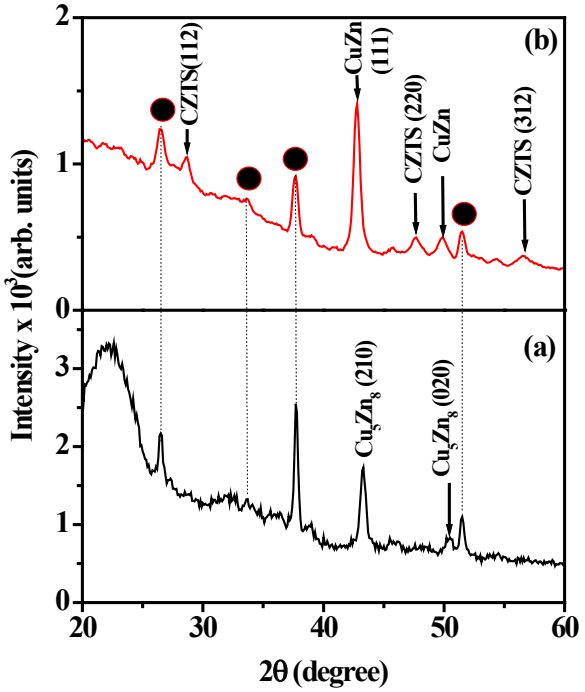

Figure 2: X-ray diffraction pattern (a) as-deposited and (b) annealed CZTS thin films at 400°C for 15 minutes.

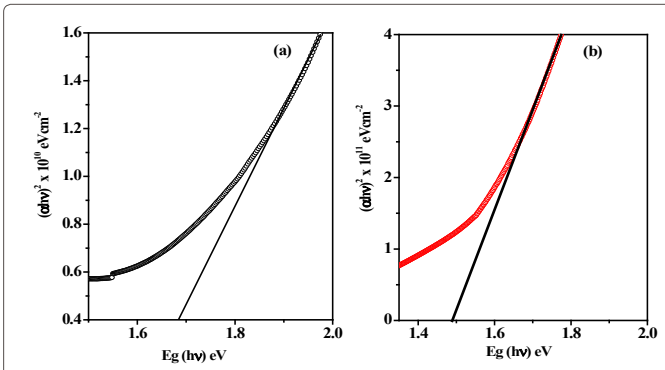

Figure 3: A plot of $(\alpha h\nu)^2$ verses Energy (hν) of (a) as-deposited and (b) annealed CZTS thin films at 400°C for 15 minutes.

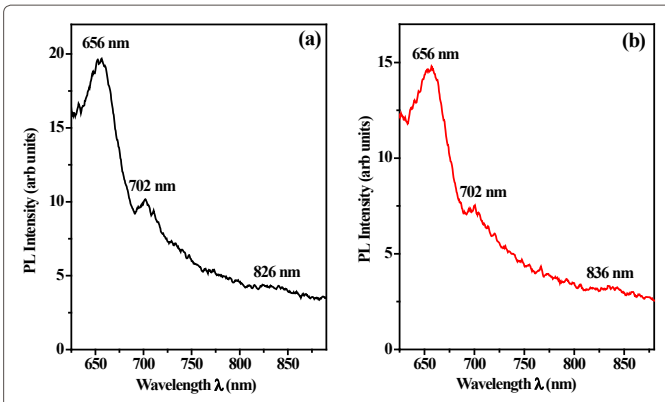

Figure 4: PL spectra of (a) as-deposited and (b) annealed CZTS thin films at 400°C for 15 minutes.

or free energy formation of Cu_5Zn_8 phase observed in as-deposited sample has been disappeared upon annealing and transformed into CuZn alloy due to the desired condition of free formation of CuZn phase.

UV-Visible spectroscopy

The optical study of as-deposited and annealed CZTS sample deposited at -1.1 V is carried out by UV- Visible –IR spectroscopy. Figure 3 depicts the $(\alpha h\nu)^2$ verses energy (hν) of (a) as-deposited and (b) annealed CZTS thin films. The optical band gap of as-deposited CZTS sample is found to be 1.68 eV. The large band gap value of as-deposited sample could be due to the short range crystallinity, presence of mixed secondary and ternary phases along with metallic phases which agrees well with XRD results. The reported band gap for Cu_2ZnSnS_4 is ~1.5 eV [1-5], however, due to variation in the chemical composition of the precursors and/or mixed surface morphology and grains size may affect on the band gap of CZTS, which can be varied in the range 1.4 eV to 1.6 eV [35,36]. Upon annealing the band gap estimated ~ 1.49 eV corresponds to CZTS. It is also noticed that after annealing the sample, the absorption intensity was found to be increased by one order of magnitude as compared to as-deposited sample.

Photoluminescence

Photoluminescence of (a) as-deposited and (b) annealed CZTS samples were studied by Perkin Elmer LS-55 Spectrophotometer and shown in Figure 4. The small shoulders observed in both as-deposited and annealed samples at 826 nm and 836 nm, respectively are associated with CZTS [1-5]. The peak exhibited around 702 nm could be associated with the ternary and quaternary alloys of CZTS. The highest intensity peak exhibited about 656 nm (1.89 eV) is associated to the formation of ternary alloys of CuZnS [37,38].

Scanning electron microscopy (SEM)

The morphology of CZTS samples were studied by scanning electron microscopy (SEM). Figures 5a and 5b depicts the SEM images of as-prepared and annealed CZTS thin films respectively. The compact and well adherent CZTS layers were deposited by electrodeposition technique at -1.1 V. It can be clearly seen from Figure 5 that the small grains are agglomerated in both as-prepared and annealed sample to form the clusters. The enhancement in the size of cluster upon annealing could be clearly seen. As both SEM images were obtained for same magnification, therefore the scale bar given in each SEM image can be used to estimate the cluster size. The particle size was found to be spherical because of the higher concentration of metallic copper and zinc. The grain size in the as-deposited film was ~ 1μm whereas after annealing it is found to be increased ~ 3-4 μm. A cauliflower like morphology has been observed in both as-deposited and annealed samples.

Energy dispersive spectroscopy (EDS)

The elemental composition of (a) as-deposited and (b) annealed CZTS films was studied by energy dispersive spectroscopy and summarized in Table 1. The elemental composition of as-deposited film is, Cu=48.28, Zn=21.88, Sn=9.43 and S=20.41, whereas after annealing it is Cu=48.03, Zn=27.89, Sn=8.82 and S=15.26. CZTS films were found to be copper and Zn rich. The sample close to the stoichiometry could be deposited by optimizing the concentration of complexing agent and/or pH and temperature of the bath (Figure 6).

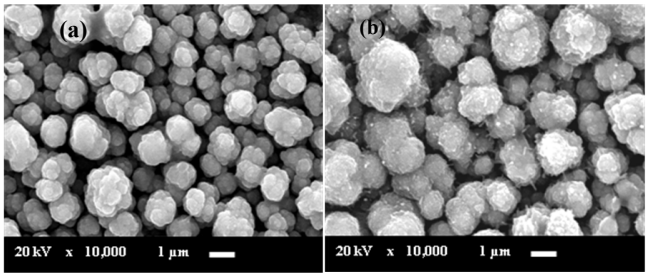

Figure 5: SEM micrographs of CZTS thin films, (a) as-deposited and (b) annealed at 400°C for 15 minutes.

Elemental Composition in At. %					
Deposition potential (V)	**Sample condition**	**Cu**	**Zn**	**Sn**	**S**
-1.1 V	As-deposited	48.28	21.88	9.43	20.41
	Annealed	48.03	27.89	8.82	15.26

Table 1: A summary of elemental compositions obtained by EDAX for as-deposited and annealed Cu_2ZnSnS_4 sample.

Current density-Voltage (J-V) measurement

The current density–voltage (J-V) measurement of as-deposited and annealed sample studied under dark condition is depicted in Figure 7. Both as-prepared and annealed CZTS sample shows Schottky behaviour under dark condition. The potential barrier, 'φ_b' was calculated by the following equation [39];

$$\varphi_b = -\frac{kT}{q}\ln\left(\frac{A^{**}T^2}{J_s}\right) \quad (6)$$

where, 'φ_b' is the barrier height, 'k' is the Boltzmann's constant, 'T' is the temperature, 'q' is the charge on electron, 'A**' is the effective Richardson's constant for CZTS (63.6 A/cm^2 K^2) [40] and 'J_s' is the reverse saturation current density. The barrier height 'φ_b' was found to ~ 0.29 eV and 0.26 eV for as-deposited and annealed CZTS sample, respectively. The barrier height φ_b is found to be decreased upon annealing the sample. This is associated with several parameters viz. the crystallinity of the layer, the formation of homogeneous mixture of ternary/quaternary alloy, presence of secondary phases, grain boundaries and nature of metal semiconductor contact.

Capacitance – Voltage (C-V) measurement

The capacitance – voltage measurement of (a) as-deposited and (b) annealed CZTS sample was performed under dark condition with frequency 100 kHz and plots are shown in Figure 8. The observed Mott-Schottky plots of both as-deposited and annealed samples were nearly similar except small change in the flat band potential. The inversion, depletion and accumulation region are observed in both as-deposited and annealed samples however, inversion region is very small. The inversion and depletion region are related to the depletion of the charge carriers whereas accumulation is related to diffusion of the charge carriers. The values of flat band potential are found to be 0.36 V and 0.30 V for as-deposited and annealed CZTS sample respectively. The carrier concentration is calculated by using the following relation [39,40].

$$N_A = \frac{2}{\varepsilon_s q}\left[-\frac{1}{\left(d\left(1/C^2\right)/dV\right)}\right] \quad (7)$$

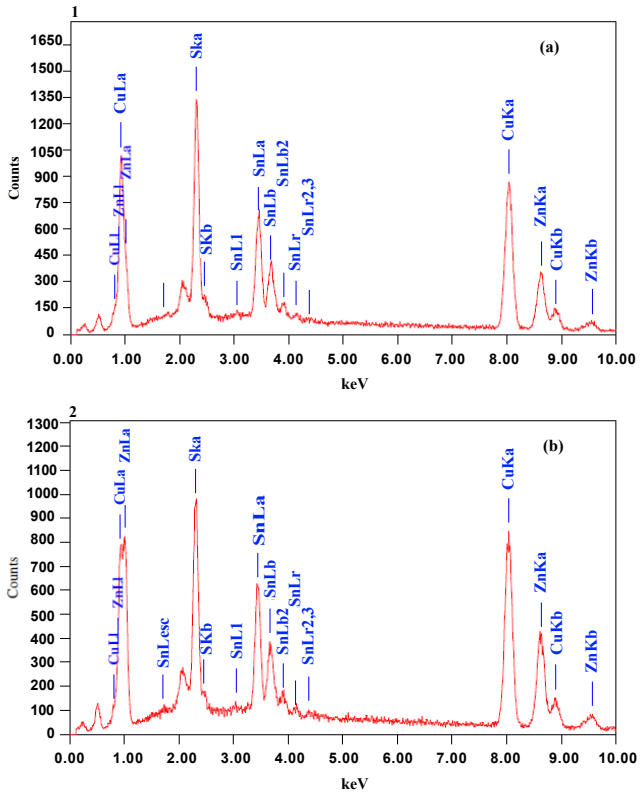

Figure 6: EDS spectra of CZTS thin films, (a) as-deposited and (b) annealed at 400°C for 15 minutes.

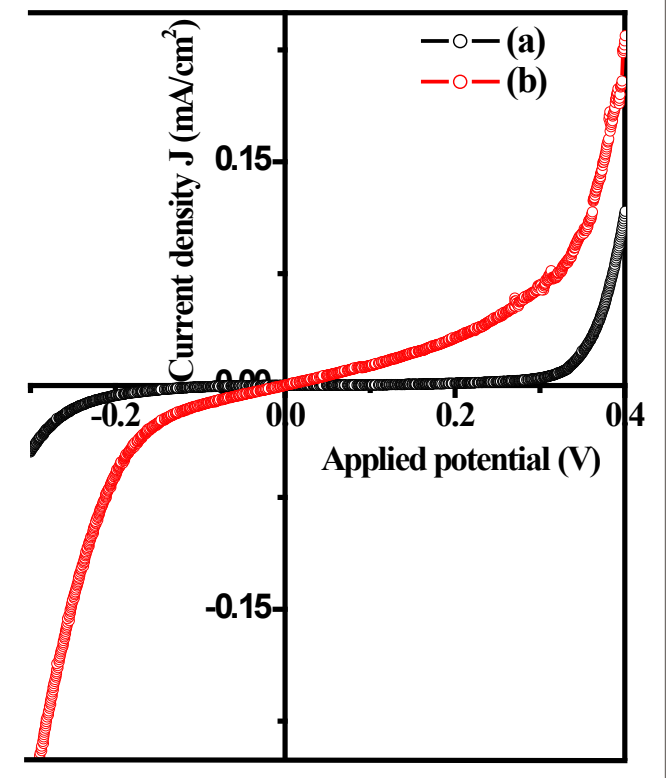

Figure 7: J-V characteristics of (a) as-deposited and annealed CZTS thin films at 400°C for 15 minutes.

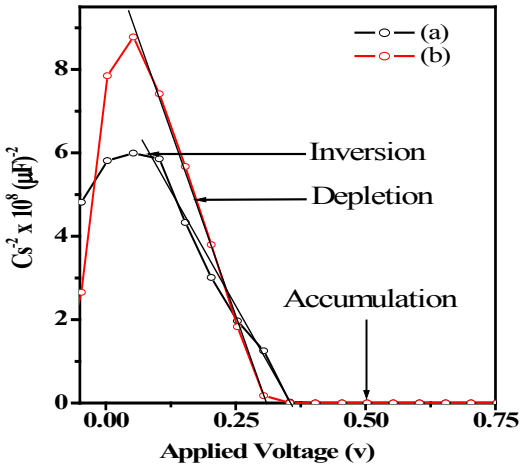

Figure 8: Mott-Schottky plots $1/Cs^2$ verses V of (a) as-deposited and (b) annealed CZTS thin films at 400°C for 15 minutes.

The value of static relative dielectric constant of CZTS material is taken 4.27 [10] for calculation of carrier concentration. The carrier concentration of the as-deposited film was found to be 1.4×10^{16} cm^{-3}. Upon annealing the carrier concentration was calculated ~ 2.4×10^{16} cm^{-3} which is very similar to that of as-deposited sample. Further optimization in annealing condition is under progress to obtain the photoactive semiconductor layers.

Conclusions

In conclusion, CZTS thin films can be deposited by low-cost electrodeposition technique. XRD results revealed (112), (220) and (312) planes corresponds to tetragonal kesterite CZTS structure. The optical band gap of the as-deposited CZTS film was found to be 1.68 eV. Upon annealing the band gap was estimated ~ 1.49 eV corresponds to CZTS which was further confirmed by photoluminescence study. Cauliflower like morphology of grain size 3 - 4 µm was observed upon annealing the CZTS sample. EDS data confirms the deposition of off stoichiometric CZTS films. The elemental composition of as-deposited film was Cu=48.28, Zn=21.88, Sn=9.43 and S=20.41, whereas, upon annealed the composition were Cu=48.03, Zn=27.89, Sn=8.82 and S=15.26. Both as-prepared and annealed CZTS sample showed Schottky behaviour under dark condition. The carrier concentration calculated from Mott-Schottky plot was found to be in the order of ~10^{16} cm^{-3}. The deposition of highly crystalline CZTS layers with desired composition close to the ideal is under progress.

Acknowledgement

One of the authors ML is thankful to University Grant Commission (UGC) for UGC-BSR fellowship.

References

1. Walsh A, Chen S, Wei S, Gong X (2012) Kesterite thin-film solar cells: advances in materials modelling of Cu_2ZnSnS_4. Adv Energy Mater 2: 400-409.
2. Grossberg M, Krustok J, Raudoja J, Timmo K, Altosaar M, et al. (2011) Photoluminescence and Raman study of $Cu_2ZnSn(Se_xS_{1-x})_4$ monograins for photovoltaic applications. Thin Solid Films 519: 7403-7406.
3. Kahraman S, Çetinkaya S, Çetinkara HA, Guder HS (2014) A comparative study of Cu_2ZnSnS_4 thin films growth by successive ionic layer adsorption–reaction and sol-gel methods. Thin Solid Films 550: 36-39.
4. Peng C, Dhakal TP, Garner S, Cimo P, Lu S, et al. (2014) Fabrication of Cu_2ZnSnS_4 solar cell on a flexible glass substrate. Thin Solid Films 562: 574-577.
5. Salome PMP, Malaquias J, Fernandes PA, Ferreira MS, daCunha AF, et al. (2012) Growth and characterization of $Cu_2ZnSn(S,Se)_4$ thin films for solar cells. Solar Energy Materials & Solar Cells 101: 147-153.
6. http://www.solar-frontier.com/eng/news/2013/C026764.html
7. Bag S, Gunawan O, Gokmen T, Zhu Y, Mitzi DB (2012) Hydrazine-processed Ge-substituted CZTSe solar cells. Chem Mater 24: 4588-4593.
8. Todorov TK, Reuter KB, Mitzi DB (2010) Photovoltaic devices: high-efficiency solar cell with earth-abundant liquid-processed absorber. Adv Mater 22.
9. Barkhouse DAR, Gunawan O, Gokmen T, Todorov TK, Mitzi DB (2012) Device characteristics of a 10.1% hydrazine-processed $Cu_2ZnSn(Se,S)_4$ solar cell. Prog Photovolt: Res Appl 20: 6-11.
10. Saha SK, Guchhait A, Pal AJ (2012) Cu_2ZnSnS_4 (CZTS) nanoparticle based nontoxic and earth-abundant hybrid pn-junction solar cells. Phys Chem Chem Phys 14: 8090-8096.
11. Zhang J, Long B, Cheng S, Zhang W (2013) Effects of sulfurization temperature on properties of CZTS films by vacuum evaporation and sulfurization method. International Journal of Photoenergy 2013: 1-6.
12. Xinkun W, Wei L, Shuying C, Shuying C, Hongjie J (2012) Photoelectric properties of Cu_2ZnSnS_4 thin films deposited by thermal evaporation. J Semicond 33.
13. Shin B, Gunawan O, Zhu Y, Bojarczuk NA, Jay Chey S, et al. (2011) Thin film solar cell with 8.4% power conversion efficiency using an earth-abundant Cu2ZnSnS4 absorber. Prog Photovolt: Res Appl 21: 72-76.
14. Washio T, Shinji T, Tajima S, Fukano T, Motohiro T, et al. (2012) 6% efficiency Cu_2ZnSnS_4-based thin film solar cells using oxide precursors by open atmosphere type CVD. J Mater Chem 22: 4021-4024.
15. Katagiri H, Jimbo K, Maw WS, Oishi K, Yamazaki M, et al. (2009) Development of CZTS-based thin film solar cells. Thin Solid Films 517: 2455-2460.
16. Fernandes PA, Salome PMP, da Cunha AF, Schubert B (2010) Cu_2ZnSnS_4 solar cells prepared with sulphurized dc-sputtered stacked metallic precursors. Thin Solid Films 519: 7382-7385.
17. Hartman K, Johnson JL, Bertoni MI, Recht D, Aziz MJ, et al. (2011) SnS thin-films by RF sputtering at room temperature. Thin Solid Films 519: 7421-7424.
18. Han J, Shin SW, Gang MG, Kim JH, Lee JY (2013) Crystallization behaviour of co-sputtered Cu_2ZnSnS_2 precursor prepared by sequential sulfurization processes. Nanotechnology 24: 095706.
19. Katagiri H, Sasaguchi N, Hando S, Hoshino S, Ohoshi J, et al. (1997) Preparation and evaluation of Cu_2ZnSnS_4 thin films by sulfurization of E•B evaporated precursors. Sol Energy Mater Sol Cells 49: 407-414.
20. He X, Shen H, Wang W, Zhang B, Dai Y, et al. (2012) Effect of donor concentration on the PTCR behavior of Y-doped $BaTiO_3$–$(Bi_1/2Na1/2)TiO_3$ ceramics. J Mater Sci: Mater Electron 24: 431.
21. Sarswat PK, Free ML (2012) A comparative study of co-electrodeposited Cu_2ZnSnS_4 absorber material on fluorinated tin oxide and molybdenum substrates. Journal of Electronic Materials 41: 2210-2215.
22. Yang K, Ichimura M (2012) Preparation, characterization, and activity evaluation of CuO/F-TiO_2 photocatalyst. International Journal of Photoenergy 2012: 1-9.
23. Pawar SM, Pawar BS, Moholkar AV, Choi DS, Yun JH, et al. (2010) Single step electrosynthesis of Cu_2ZnSnS_4 (CZTS) thin films for solar cell application. Electrochimica Acta 55: 4057-4061.
24. Zhang X, Shi X, Ye W, Ma C, Wang C (2009) Electrochemical deposition of quaternary Cu_2ZnSnS_4 thin films as potential solar cell material. Appl Phys A 94: 381-386.
25. Bhattacharya RN, Kim JY (2012) Cu-Zn-Sn-S thin films from electrodeposited metallic precursor layers. The Open Surface Science Journal 4: 19-24.
26. Kamoun N, Bouzouita H, Rezig B (2007) Fabrication and characterization of Cu_2ZnSnS_4 thin films deposited by spray pyrolysis technique. Thin Solid Films 515: 5949-5952.
27. Kumar YBK, Babu GS, Bhaskar PU, Raja VS (2009) Preparation and characterization of spray-deposited Cu_2ZnSnS_4 thin films. Solar Energy Materials and Solar Cells 93: 1230-1237.

28. Slupska M, Ozga P (2014) Electrodeposition of Sn-Zn-Cu alloys from citrate solutions. Electrochimica Acta 141: 149-160.

29. Khalil MI, Bernasconi R, Magagnin L (2014) CZTS layers for solar cells by an electrodeposition-annealing route. Electrochimica Acta 145: 154-158.

30. Valdes M, Modibedi M, Mathe M, Hillie T, Vazquez M (2014) Electrodeposited Cu_2ZnSnS_4 thin films. Electrochimica Acta 128: 393-399.

31. Ge J, Jiang J, Yang P, Peng C, Huang Z, et al. (2014) A 5.5% efficient co-electrodeposited ZnO/CdS/Cu_2ZnSnS_4/Mo thin film solar cell. Solar Energy Materials & Solar Cells 125: 20-26.

32. Lee SG, Kim J, Woo HS, Jo Y, Inamdar AI, et al. (2014) Structural, morphological, compositional, and optical properties of single step electrodeposited Cu_2ZnSnS_4 (CZTS) thin films for solar cell application. Current Applied Physics 14: 254-258.

33. Pandey RK, Sahu SN, Chandra S (1996) Handbook of semiconductor electrodeposition. CRC Press, USA.

34. Walsh A, Chen S, Wei S, Gong X (2012) Kesterite thin-film solar cells: advances in materials modelling of Cu_2ZnSnS_4. Adv Energy Mater 2: 400-409.

35. Han J, Shin SW, Gang MG, Kim JH, Lee JY (2013) Crystallization behaviour of co-sputtered Cu_2ZnSnS_2 precursor prepared by sequential sulfurization processes. Nanotechnology 24: 095706.

36. Zaberca O, Oftinger F, Chane-Ching JY, Datas L, Lafond A, et al. (2012) Surfactant-free CZTS nanoparticles as building blocks for low-cost solar cell absorbers. Nanotechnology 23:185402.

37. Kitagawa N, Ito S, Nguyen D, Nishino H (2013) Copper zinc sulfur compound solar cells fabricated by spray pyrolysis deposition for solar cells. Natural Resources 4: 142-145.

38. Yildirim MA, Ates A, Astam A (2009) Annealing and light effect on structural, optical and electrical properties of CuS, CuZnS and ZnS thin films grown by the SILAR method. Physica E 41: 1365-1372.

39. Sze SM, Poplai HS (1983) Physics of semiconductor devices. 3rd Edn., Wiley Eastern Limited, New Delhi, India.

40. Rakhshani AE, Thomas S (2015) Cu2ZnSnS4 films grown on flexible substrates by dip coating using a methanol-based solution: electronic properties and devices. Journal of Electronic Materials 44: 4760-4768.